

ESTIMATION OF THE SPACE SHUTTLE ROLLOUT FORCING FUNCTION

George H. James III
Structures & Dynamics
Branch – ES2
NASA Johnson Space
Center
2101 NASA Rd. 1
Houston, TX 77058

Thomas Carne
Sandia National
Laboratories
Albuquerque, NM

Kenny Elliott
NASA Langley
Research Center
Langley, VA

Bruce Wilson
Lockheed Martin Space
Operations
Houston, TX

ABSTRACT

The Space Shuttle Vehicle is assembled in the Vertical Assembly Building (VAB) at Kennedy Space Flight Center in Florida. The Vehicle is stacked on a Mobile Launch Platform (MLP) that weighs eight million pounds. A Crawler Transporter (CT) then carries the MLP and the stacked vehicle (12 million pounds total weight) to the launch complex located 5 miles away. This operation is performed at 0.9 mph resulting in a 4.5-hour transport. A recent test was performed to monitor the dynamic environment that was produced during rollout. It was found that the rollout is a harmonic-rich dynamic environment that was previously not understood.

This paper will describe work that has been performed to estimate the forcing function that is produced in the transportation process. The rollout analysis team has determined that there are two families of harmonics of the drive train, which excite the system as a function of CT speed. There are also excitation sources, which are random or narrow-band in frequency and are not a function of CT speed. This presentation will discuss the application of the Sum of Weighted Accelerations Technique (SWAT) to further refine this understanding by estimating the forces and moments at the center-of-mass.

INTRODUCTION

The Space Shuttle vehicle is comprised of several major elements during launch: the manned Orbiter with the Space Shuttle Main Engines (SSME's), two reusable Solid Rocket Boosters (SRB's), and the External Tank (ET) that connects everything together. This entire three million pound stack is mounted to an eight million pound Mobile Launch Platform (MLP) and carried to the launch pad by the one million pound Crawler Transporter (CT). Figure 1 shows this process underway at the typical rollout speed of 0.9 miles per hour (mph).

The rollout has been considered a relatively benign environment during most of the life of the Shuttle System. However, as the System ages and more emphasis has been placed on understanding the fatigue characteristics, this assumption has become a *subject for validation*. As the technical community began to study this environment, the rollout forcing function was found to contain a fairly rich spectrum.

A series of tests were performed in November of 2003 to develop the data necessary to understand the dynamic environment of Rollout and the response of the Space Shuttle Vehicle [1, 2]. The hardware used in these tests consisted of an MLP and a CT as well as a partial stack. This partial stack consisted of two SRB's and a crossbeam forming the upper interface. This crossbeam is a component that is normally embedded in an ET. Figure 2 shows the configuration. It should be noted that this configuration contains all but 250,000 pounds of the 12 million pound stack. However, the missing Orbiter and ET do add significant stiffness and dynamics to the stack.

Data was acquired on the system at several different speeds (0.5, 0.6, 0.7, 0.8, and 0.9 mph). There were nine channels of acceleration (three sets of triaxial sensors) acquired on each SRB (18 total). There were an additional 20 locations (60 channels) with triaxial measurements on the MLP. These are the 78 channels of data that were of most interest in this work. Additionally the SRB/MLP interface was monitored with additional strain gauges and the CT had nine additional locations with triaxial measurements. Wind speed and direction, CT speed, and pressures in the hydraulics that lift the MLP were also monitored [1].



Figure 1. Space Shuttle Stack During Rollout



Figure 2. Partial Stack During Rollout Testing

Significant follow-on work has been underway to develop and apply the Rollout forcing functions studied in these tests to predict vehicle response [3-4]. The work reported herein represents one aspect of these efforts. Specifically, the authors have been using a force reconstruction technique developed at Sandia National Laboratories called the Sum of Weighted Acceleration Technique [5] or SWAT to estimate the forcing function operating on the MLP and partial stack during the Rollout tests. An estimate of the forcing function will be used to understand the causes and effects of the transportation environment. It is also hypothesized that the partial stack forcing function will be very similar to the full stack forcing function. This is primarily due to the fact that the dynamics of the stack will not significantly affect the input forces. The alternative (and primary analysis approach for full stack rollout) is to use a set of base drive accelerations to drive the system. This approach is initially easier to implement and has been used historically in this situation. However the acceleration inputs will not be directly transferable from the partial stack rollout test to the full stack vehicle rollout because of the changing dynamics of the stack due to the missing mass and stiffness and the resulting modal differences [4].

SWAT FORCES AT THE CENTER OF GRAVITY

SWAT combines measured accelerations multiplied by scalar weights to produce estimated forces. The weights, which appropriately sum the accelerations, are chosen to filter out the system dynamics, retaining the acceleration of the center-of-mass as described by the rigid body modes of the system. Knowledge of the mass and mass moments of inertia then allows Newton's law to be applied to estimate the forcing functions summed together at the center of gravity (CG) [5].

$$\underline{F}_{CG} = M \underline{a}_{CG}; \quad (1)$$

Where \underline{F}_{CG} is the six Degree-Of-Freedom (DOF) CG force vector, M is the rigid body mass matrix, and \underline{a}_{CG} is the acceleration vector at the CG. Reference [6] covers the development of SWAT in detail. However, an abbreviated development of the theory begins with the relationship that the measured acceleration time histories (\underline{a}) can be described as a summation of accelerations of modal participations (\ddot{p}_j) and mode shapes ($\underline{\phi}_j$) as shown in Equation 2:

$$\underline{a}(t) = \sum_i \ddot{p}_j(t) \underline{\phi}_j. \quad (2)$$

After converting the standard structural equations of motion into modal space and assessing only the contributions of the rigid body modes, the stiffness and damping properties of the structure vanish. The inertial properties of the structure describe the response to externally applied forces as shown in equation (3):

$$m_r * \ddot{p}_r(t) = \underline{\phi}_r^T * \underline{f}(t); \quad (3)$$

Where:

m_r Is the mass property of a rigid body mode,

\ddot{p}_r Is the modal acceleration of the rigid body mode,

$\underline{\phi}_r$ Is the rigid body mode shape,

$\underline{f}(t)$ Is the external force vector.

Equation (3) is a manifestation of the basic premise of reference (6): "Knowledge of the rigid-body modal coordinates is sufficient to determine the sum of all externally applied forces".

As mentioned previously, a weighted summation of the accelerations will be used to create a generalized DOF as in equation (4):

$$s_i(t) = \sum_k w_{ik} a_k(t) = \underline{w}_i^T * \underline{a}(t); \quad (4)$$

Where s_i is a generalized coordinate and \underline{w}_i is a weight vector. Substituting (2) into (4) and rearranging, the following description of the generalized coordinate is produced:

$$s_i(t) = \sum_k \ddot{p}_k(t) \{ \underline{w}_i^T * \underline{\phi}_k \} \quad (5)$$

Now the proper selection of weights will allow the generalized coordinate (s) to be interpreted as an acceleration of a DOF of the center-of-mass (a_{CG}). Specifically, the weights must be chosen such that the product of the weights with all retained elastic modes and all non-desired rigid body modes are null. The weight matrix is normalized such that the product with the desired rigid body DOF is 1.0 as shown in equation (6):

$$\underline{w}_i^T * \underline{\phi}_{ik} = \delta_{ik}; \quad (6)$$

Where δ_{ik} is the delta function which is only a non-zero value (1.0) if $i = k$. The user must be careful in the choice of sensor locations and the subset of included modes to assure that equation (6) can be solved for the weights of interest. It is critically important that the mode shape matrix not be singular or ill-conditioned with respect to the measurement locations. Reference [6] and other papers by the SWAT developers should be used to develop a proper understanding of the intricacies of determining SWAT weights.

Substituting (6) into (5) and equating to (3) results in:

$$\ddot{s}_i(t) = \ddot{p}_i(t) = \underline{w}_i^T \underline{a}(t) = \underline{\phi}_i^T \underline{f}(t) / m_i. \quad (7)$$

And finally equation (7) and equation (1) can be combined after multiplying (7) by the mass property and relating the sum of the forces at the CG:

$$F_{CG_i} = \underline{\phi}_i^T \underline{f}(t) = m_i a_{CG_i} = m_i \underline{w}_i^T \underline{a}(t). \quad (8)$$

Note that if the rigid body mode of interest is a translation mode, then the mass property is the total mass of the system and the force is the sum of all external forces in that direction. If the rigid body mode is a rotational mode, then the mass property is the mass moment of inertia about the axis of rotation and the force is the sum of all moments about that same axis. Hence, six sets of weights and rigid body properties are required to develop a complete description of the sum of all external forces.

SWAT FORCES FOR THE PARTIAL STACK/MLP OPERATING AT .9 MPH

SWAT forces at the CG of the partial stack were developed using 78 accelerometer channels on the SRB's and the MLP. The weights were developed using the six rigid body modes along with the first ten flex modes of the system (up to 4.22 Hz) as produced by the free-free model of the partial stack system. It should be noted that the CT was not modeled in the system and is considered the source of the input forces. Figures 3 – 8 provide these six SWAT traces (three forces and three moments) while the system is moving at .9 mph. The upper plot is the time domain and the lower plot is the associated autospectrum. The force plots (Figures 3-5) suggest that net forces in the range of 100,000 to 200,000 lbs are imposed on the system. Although several peaks are seen in Figures 3-8, the critical first harmonics at .56 and .9 Hz are visible as well as the dominant peak at 2.7 Hz [1].

SWAT FORCE COMPARISON TO JEL FORCES AS ESTIMATED FROM PRESSURES

The Space Shuttle System CT includes a hydraulic system that lifts the MLP and vehicle stack called the Jacking, Elevation, and Leveling (JEL) system. There are eight independent pressure systems (two sets of two 20 inch diameter pistons at each corner of the CT). During the Partial Stack Rollout tests, the pressures in these hydraulic systems were measured. This can be directly related to the forces in the X direction (vertical). These forces were summed and scaled to convert pressure to force (assuming that each piston is 20 inches in diameter). The comparison between this measurement of X force and that developed from SWAT is shown in Figure 9. Note that the overall magnitude of the JEL force is very similar to that of the SWAT force at the dominant 2.7 Hz harmonic. Also, the relative character of the traces looks very similar. Figure 10 provides the autospectrum representation of the time domain data in Figure 9. The frequency representation of the data supports the observation that the character of the data is very similar although there are differences. However, the magnitudes in Figure 10 are squared functions and the differences are accentuated. The trend seen in the Figure 10 comparisons could be due to model errors (which will manifest themselves in incorrect SWAT weights) or an incomplete understanding of the conversion of JEL pressures to force. Also, to further enhance the frequency fidelity of the SWAT forces, more sensors or a more linearly independent set of measurement locations would have to have been utilized.

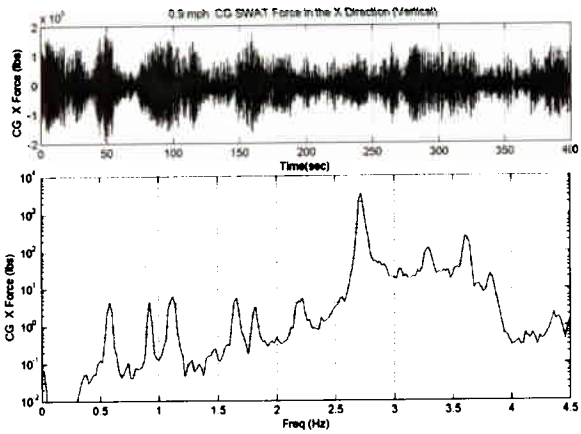


Figure 3. CG SWAT Force in the X Direction (Vertical)

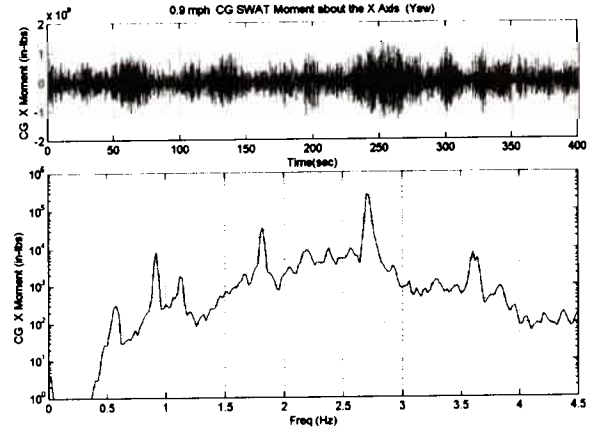


Figure 6. CG SWAT Moment about X (Yaw)

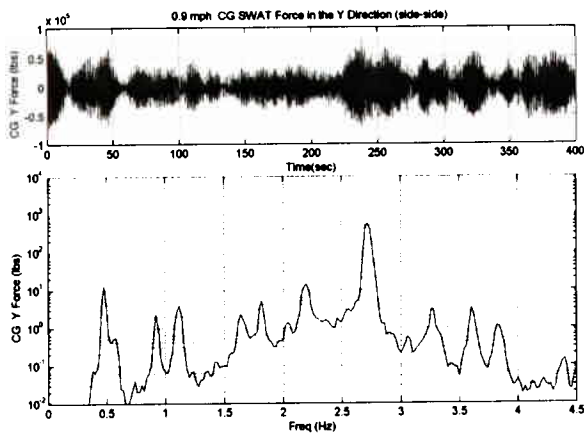


Figure 4. CG SWAT Force in the Y Direction (Lateral)

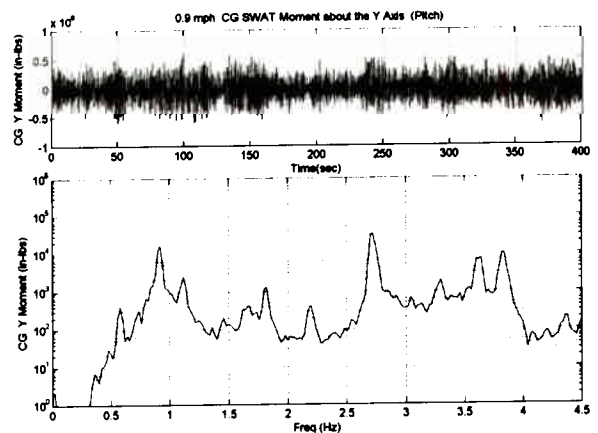


Figure 7. CG SWAT Moment about Y (Pitch)

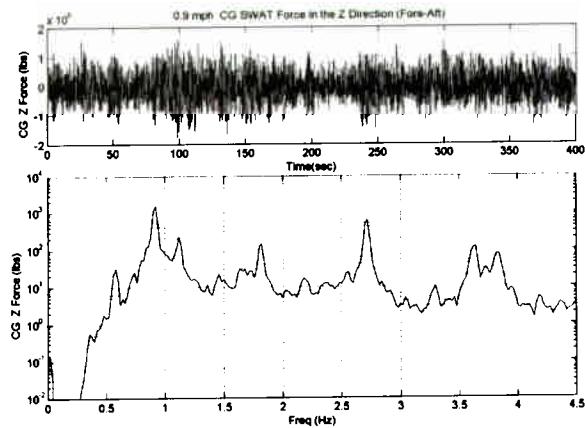


Figure 5. CG SWAT Force in the Z Direction (Travel)

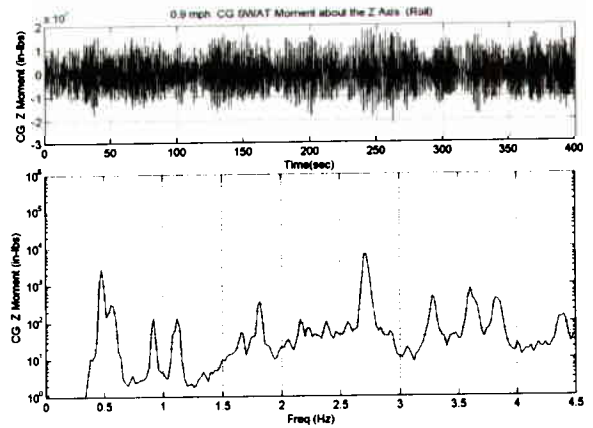


Figure 8. CG SWAT Moment about Z (Roll)

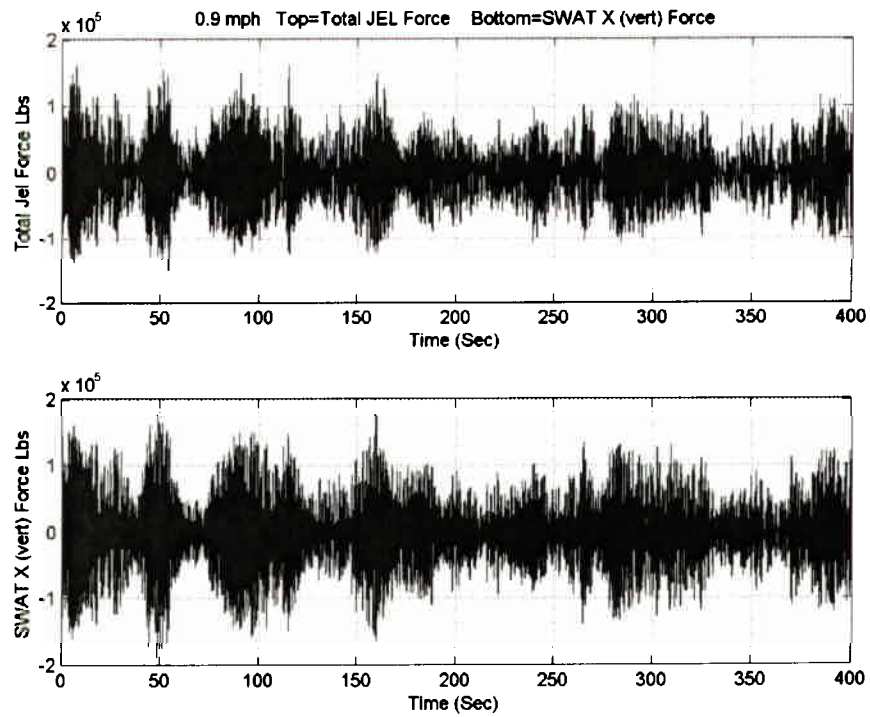


Figure 9. CG SWAT X Force and Sum of All JEL Forces (As Estimated from Pressures) – Time Domain

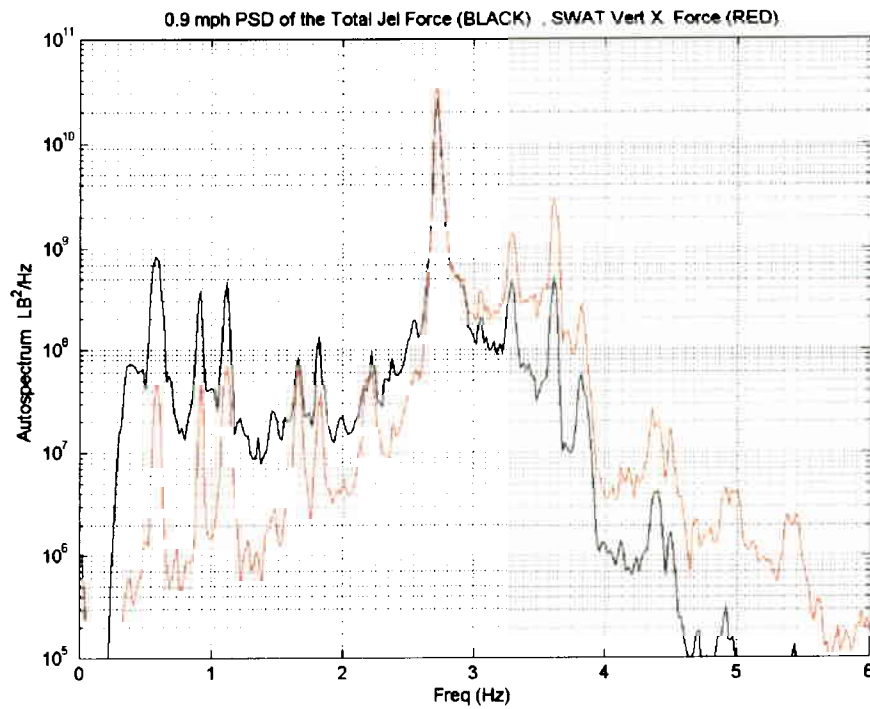


Figure 10. SWAT X Force (Red) and Sum of All JEL Forces as Estimated from Pressures (Black) – Frequency Domain

MODEL RESPONSE USING SWAT FORCE INPUTS AT .9 MPH

The real test of goodness for the SWAT forces comes from a comparison of the measured accelerations to the analytical accelerations from a NASTRAN model driven by the SWAT forces. There are two sources of potential error that must be considered when performing such a comparison. First, the NASTRAN model is not expected to be a perfect representation of reality. The complexity of the structure and the lack of ability to perform extensive modal tests/model correlation limit the ability of the model to exactly match reality. SWAT is somewhat immune to this issue, as the technique does not require an exact match of modal frequency. The retained modes of the actual system only have to be spanned by the retained modes of the model. However, the model inconsistencies will still be a factor when using it to predict structural responses. Second, the SWAT forces must be applied at the CG. Since the model does not have a load-carrying node at that location, rigid links to the actual force interface locations (the four CT/MLP interface points) are required. This artificially increases the stiffness of the MLP. It is also important to note that the system modes used to develop these SWAT weights were estimated from a model without the CG node or the rigid links. Figures 11 and 12 illustrate the range of these comparisons.

Figure 11 is an example of the least favorable comparisons and is typical of measurements from the MLP. This location is on the left side of the MLP as the vehicle rolls toward the pad. Note that there is significant variation at the lower frequencies in the Y (lateral) and Z (travel) directions. At the higher frequencies, some peaks are captured well, but the general trend is a lower analytical response. It should be noted that the MLP model has undergone less rigor in dynamic testing and correlation than the flight elements of the Space Shuttle System. This situation is further degraded by the application of false rigid body links that were needed to apply the SWAT forces to the CG of the model. On the positive side, the contribution of the MLP to the elastic modes of the system is limited until 4.5 Hz.

Figure 12 provides a much more positive result. These data are in the Z direction (direction of travel) at the top of the right-hand SRB. This result is typical for the SRB locations in this test. Note that the test and analysis correlate well. In fact this is an important result as this location is very near one of the attach points for the ET/Orbiter and is potentially more indicative of the fidelity that a full stack analysis might have. The SRB's have been subjected to much more diagnostic testing and model correlation than the MLP model. Also, at these frequencies and excitation levels, the SRB is a simpler structure to model than the MLP.

SWAT-ESTIMATED FORCING FUNCTION AS A FUNCTION OF ROLLOUT SPEED

Rollout data was acquired for constant speed rollouts at .5, .6, .7, .8, and .9 mph. Figures 13-18 are plots of the six SWAT CG load components vs. rollout speed. The frequency content is almost entirely comprised of harmonics of 0.59 times the rollout speed and harmonics of 0.975 times the rollout speed (Reference [1]). Both families of harmonics overlay for the harmonic running from 1.3 Hz thru 2.7 Hz in the plots, making that harmonic the dominant source of excitation. While the specifics of the excitation source for the two harmonic families are not fully understood, the plots are a testament that the two harmonic families do exist. The harmonic excitation source may involve some interaction between the crawler tracks and the ground. The peak at the 2.7 Hz harmonic while traveling at .9 mph shows a significant increase in the X direction (vertical) as this speed is approached (Figure 13). This harmonic appears dominant for a wider range of speeds in the Y direction (lateral – Figure 14) and the X moment (yaw – Figure 16). The Z direction (travel – Figure 15), the Y moment (pitch – Figure 17), and Z moment (roll – Figure 18) show strong contributions at the fundamental harmonics. In general, the contributions of the system elastic modes have been effectively filtered out by SWAT (although the peak at .8 mph in Figure 18 may be an exception).

CONCLUSIONS

SWAT has been used to extract forcing function estimates from the acceleration measurements of the Rollout Test data. This was accomplished by utilizing the free-free model of the partial stack attached to the MLP. The modes for this system were used to develop the SWAT weights. In an ideal world, the weights would have been developed from test data in the modal, frequency, or time domain. However, performing a free-free test on the 11.7 million pound system is cost and technology prohibitive. Hence, the user must be aware that model errors may be present in the estimated SWAT forces. Also in an ideal world, pre-test analysis would have been performed to place the sensors at locations to allow the selection of SWAT weights from the largest set of modes as possible. However, in spite of these shortcomings, the resulting forces are able to reproduce many of the necessary aspects of the real forcing function such as frequencies and amplitudes of the critical harmonics; variability with respect to the CT speed; lack of modal frequency content; and reproduction of critical response accelerations.

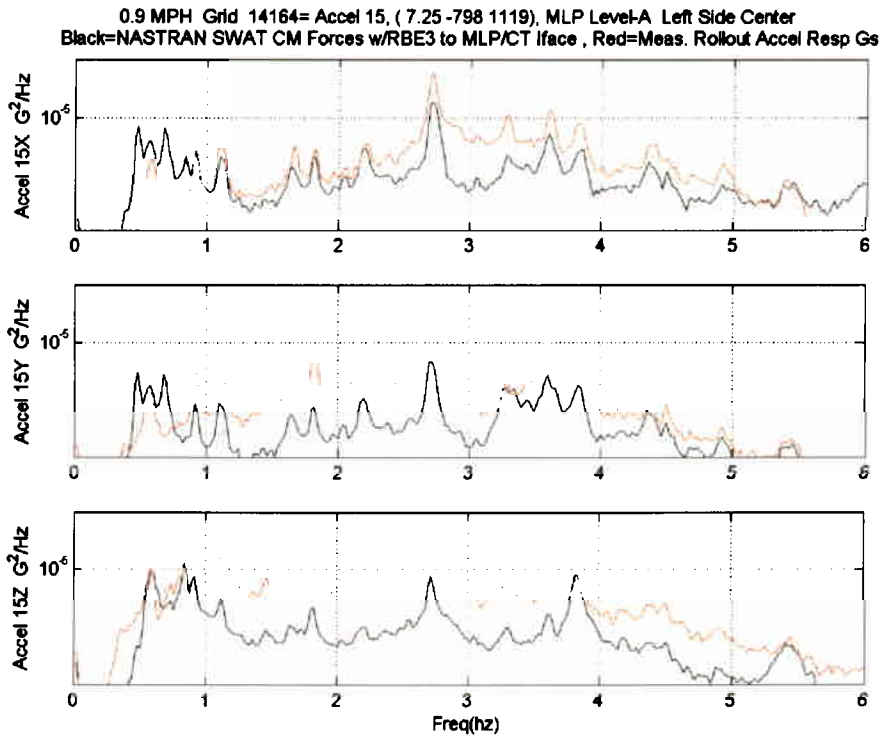


Figure 11. NASTRAN Results With SWAT Force Inputs (Black) vs. Measured Accelerations (Red) – X, Y, Z @ Left Side of MLP

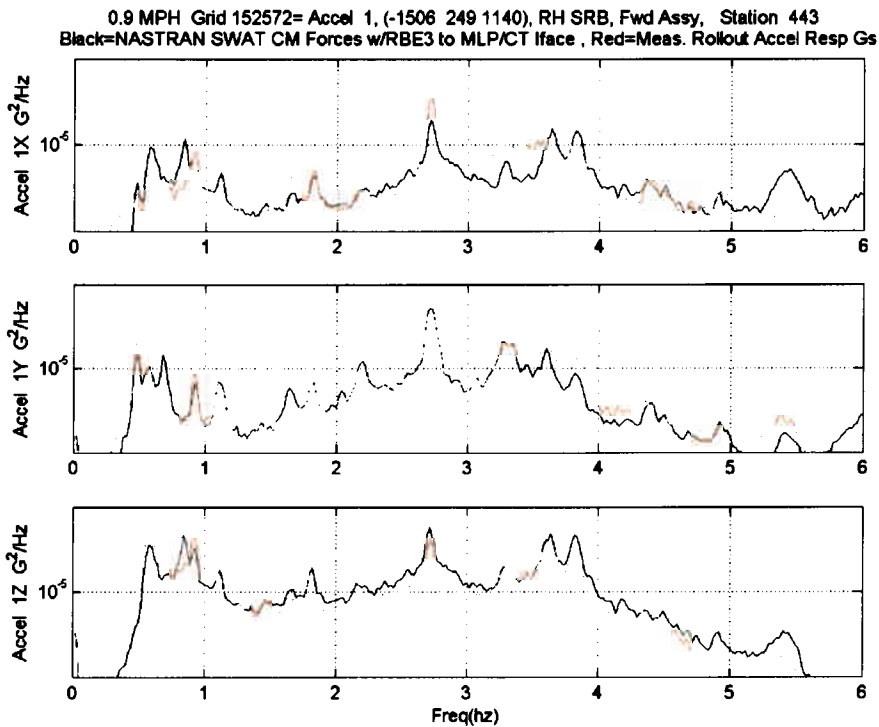


Figure 12. NASTRAN Results With SWAT Force Inputs (Black) vs. Measured Accelerations (Red) – X, Y, Z @ Top of Right SRB

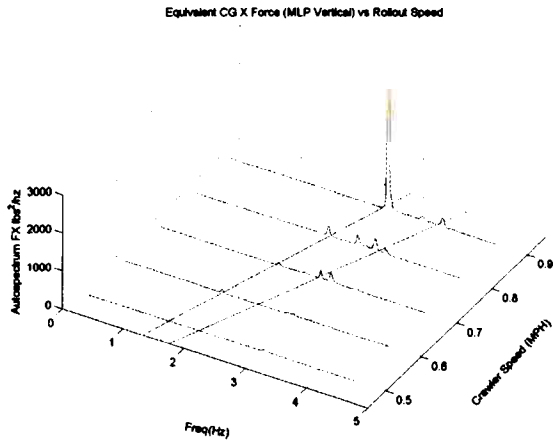


Figure 13. SWAT CG X Force (Vertical) vs. Speed

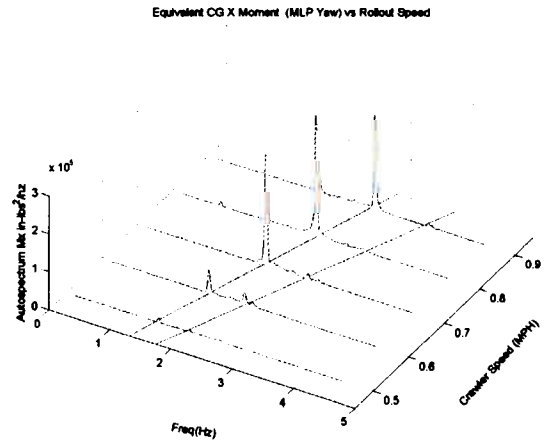


Figure 16. SWAT CG XX Moment (Yaw) vs. Speed

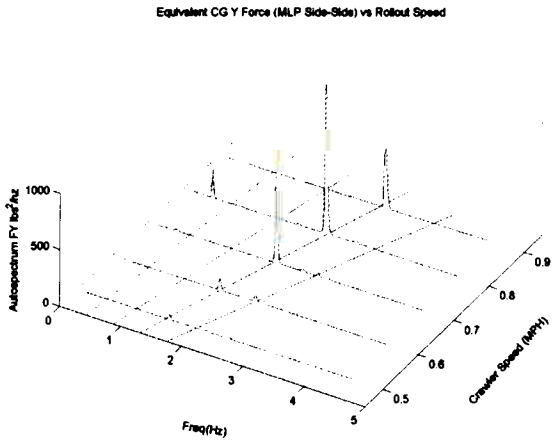


Figure 14. SWAT CG Y Force (Lateral) vs. Speed

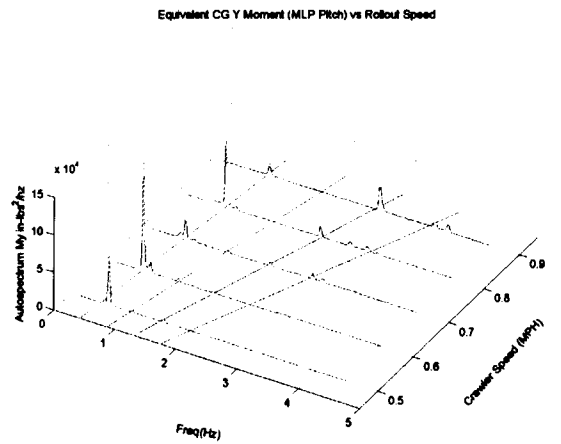


Figure 17. SWAT CG YY Moment (Pitch) vs. Speed

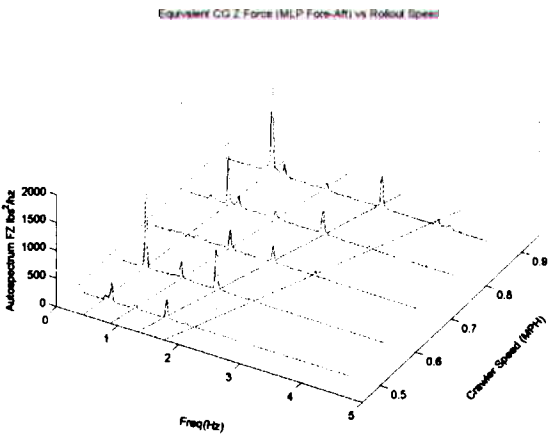


Figure 15. SWAT CG Z Force (Travel) vs. Speed

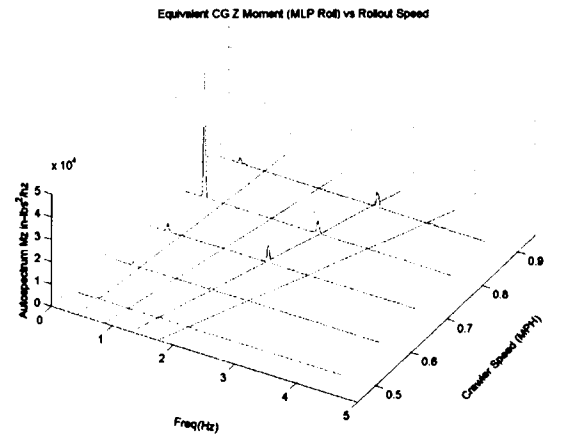


Figure 18. SWAT CG ZZ Moment (Roll) vs. Speed

The summation and scaling of the JEL system pressures produce an alternative estimation of one of the estimated SWAT forces. This provides a unique check of the estimated SWAT forces. The SWAT force reproduced the major harmonics of the JEL force. However, it was found that the overall amplitudes of the SWAT forces were off by an approximate factor of two. There was also a trend of a higher SWAT force at higher frequencies. However, this is not surprising as only a limited number of modes were used in the generation of the SWAT weights.

The final verification of the applicability of rollout forces involves the response output of the system model when driven with the extracted forces. The work reported herein compared model output at .9 mph to measured accelerations. The responses on the SRB's were matched well, while the MLP responses were more deficient. This could be due to model errors or to the limitations in the modal response of the SWAT forces. The SRB-dominated modes begin at .45 Hz, while the MLP-dominated modes begin at 4.5 Hz. Since the SWAT weights were necessarily skewed to the lower frequencies, it is not unexpected that the SRB accelerations were matched with higher fidelity. It should also be noted that some elements of the Shuttle Vehicle that were not present during the test (the ET and the Orbiter) are attached to the SRB's and not the MLP. Hence, the reproduction of the SRB responses is considered a critical indicator of goodness. It should also be noted that the SRB models are more highly correlated. There have been multiple opportunities during ground tests, static firings, and flight to verify SRB modes. The dynamics of the MLP have not been studied to the extent of the flight elements until recently. It should also be noted that the direct application of SWAT forces, requires artificial stiffness must be added to the MLP to connect a CG node to the actual force interface locations. This degrades the fidelity of the MLP model even further.

The SWAT approach was used to generate forcing functions at multiple speeds. This allows a clear visualization of the increasing force magnitudes that are generated as the speed of the rollout is increased. This information will be coupled with knowledge of full stack modal frequency locations to assess the level of resonance excitation that is expected during a typical rollout. This information will also be extremely helpful in choosing a rollout speed that will assure that fatigue life of Shuttle components are not affected by rollout.

There are several follow-on activities suggested by this work. First, the six DOF SWAT forces need to be decomposed into equivalent forces at the MLP/CT interface points. This will more closely model reality and negate the need to add artificial stiffness to the MLP model. Second, an analytical representation of the forcing function needs to be developed. Amplitude, phase, and input shape parameters as a function of CT speed need to be developed. This will then allow the forcing function to be tailored for use on analysis of the historical full stack rollouts, which is the third follow-on activity.

There are two more follow-on activities that are suggested and should be pursued as time allows. The system used for all of the rollout analysis to date does not include a model of the CT. However, the testing has shown that the CT is an active part of the system. SWAT forces should be generated for a system that includes a model of the CT. A comparison to the current SWAT forces will then allow an assessment of the need to include such a model in subsequent rollout analyses. And finally, the most import utility of the derivation of forcing functions is to understand the genesis of these forces and to determine if they have or will change over time.

ACKNOWLEDGMENTS

There are a multitude of individuals and organizations that have made the Rollout Test and analysis activities a success. The Space Shuttle Loads Panel has been the technical community within which all of these activities have been performed. The Space Shuttle System Engineering and Integration Office continues to manage and fund these activities. The Space Shuttle Program Managers have had the difficult task of balancing the technical recommendations and the larger program needs and have allowed this work to proceed. The success of the testing and the quality of the data have been made possible by the dedication of the NASA Kennedy Spaceflight Center personnel who assisted, enabled, and led the test activities. NASA Langley Research Center, NASA Marshall Spaceflight Center, Sandia National Laboratories, Boeing, and NASA Johnson Spaceflight Center all have provided test equipment and personnel for the test. However, the most critical individual to the historical and future activities related to the understanding and control of the rollout environment is the Space Shuttle Program's Jene Richart. He has been the critical link in all phases of NASA's response to the rollout issue.

REFERENCES

- [1] K. Elliott, R. Buehrle, and G. James, "Space Shuttle Transportation (Rollout) Loads Diagnostics", Proceedings of the 23rd International Modal Analysis Conference, Orlando, FL, Jan. 31 – Feb. 3, 2005.
- [2] R. Buehrle and K. Kappus, "Operating Deflection Shapes for the Space Shuttle Partial Stack Rollout", Proceedings of the 23rd International Modal Analysis Conference, Orlando, FL, Jan. 31 – Feb. 3, 2005.
- [3] J. Townsend, I. Torres, and K. Smalley, "Shuttle Rollout Base Drive Dynamic Analysis for Derivation of Load Fatigue Spectra", Proceedings of the 23rd International Modal Analysis Conference, Orlando, FL, Jan. 31 – Feb. 3, 2005.
- [4] S. Del Basso, J. Dolenz, and L. Wilson, "Space Shuttle Partial Stack Rollout Test Analytical Correlation in Support of Fatigue Load Development", Proceedings of the 23rd International Modal Analysis Conference, Orlando, FL, Jan. 31 – Feb. 3, 2005.
- [5] T. Carne, V. Bateman, and R. Mayes, "Force Reconstruction Using a Sum of Weighted Accelerations Technique", Proceedings of the 10th International Modal Analysis Conference, San Diego, CA, Feb. 3-7, 1992.